Korean J. Chem. Eng., 33(5), 1736-1742 (2016)
DOI: 10.1007/s11814-016-0009-6

pISSN: 0256-1115
eISSN: 1975-7220

Anticorrosive properties of olive oil polyurethanamide/ZnO biocomposite coatings

Manawwer Alam*,†, Naser Mohammed Alandis, Eram Sharmin***, Fahmina Zafar****, and Mohammad Asif Alam*****

*Research Centre-College of Science, King Saud University, P. O. Box 2455, Riyadh 11451, Saudi Arabia
**Department of Chemistry, College of Science, King Saud University, P. O. Box 2455, Riyadh 11451, Saudi Arabia
***Department of Pharmaceutical Chemistry, College of Pharmacy, Umm Al-Qura University, P. O. Box 715, Makkah Al-Mukarramah, 21955, Saudi Arabia
****Inorganic Materials Research Laboratory, Department of Chemistry, Jamia Millia Islamia, New Delhi 110 025, India
*****Advanced Manufacturing Institute, Center of Excellence in Engineering Materials, King Saud University, P. O. Box 800, Riyadh-11421, Saudi Arabia
(*Received 16 October 2015 • accepted 7 January 2016*)

Abstract−Olive oil based polyurethanamide/ZnO biocomposites were prepared by energy efficient microwave irradiation technique. The biocomposites showed good coating properties: scratch resistance, impact resistance, adhesion and flexibility retention. The corrosion studies carried out by potentiodynamic polarization measurements exhibit inhibition efficiency of 99.99% in 5% NaCl, 99.99% in 3.5% HCl, and 99.94% tap water, respectively. The overall approach is significant as it focuses on the utilization of vegetable oil, a sustainable material, polyurethanamide, synthesized through an energy efficient technique, at lower temperature, in lower reaction time, promoting value addition through simple chemistry. The coatings provide corrosion protection by barrier action.

Keywords: Olive Oil, Polyurethane, Coatings, ZnO, Potentiodynamic

INTRODUCTION

Polyurethanamide (PUA) is an emerging class of polymer from vegetable oils [VO]. Here urethane and amide linkages are present in the same polymeric chain. VO based PUA is prepared by the addition reaction between -OH groups of diol fatty amide (DFA) and -NCO groups of a diisocyanate. The urethane linkages enhance abrasion resistance, toughness, and chemical resistance, providing protection in outdoor services, while the amide linkages enhance alkali resistance, thermal stability and tensile strength [1-4]. Karak et al. synthesized PUA by chemical reaction of Nahar oil based DFA and toluene-2,4-diisocyanate [TDI] in presence of dibutyltin-dilaurate (catalyst) and polyethylene glycol (chain extender) [5]. Ahmad et al. synthesized PUA by one shot technique using DFA from Linseed, *Pongamia glabra*, Castor oil and TDI for corrosion protective coatings [6-8]. In their latest work they have modified *Pongamia*, Linseed oil derived PUA through the incorporation of metal and metalloid (boron and silicon) with improved performance relative to the virgin PUA [9-12].

For advanced applications, the modification of polymers as nanocomposites (PNC) with very low loading (less than 5 vol%) of well dispersed nanosized fillers gets much attention due to their unique mechanical, thermal, and optical properties [13]. The properties of PNC depend on the particle size, shape and loading, and also the distribution of (fillers) nanoparticles in polymer with good adhesion at the interface [14]. There are various inorganic nanoscale fillers such as nanoclay [15,16], nanosilica [12], nanosilver [17], aluminum oxide [18], titanium dioxide [19,20], zinc oxide (ZnO) [13], nano-ZrO2 [21], nano-iron oxide [22,23], graphene [24] and carbon nanotube [25] with varying particle sizes along with surface modifications, that have been used in very low % to improve the overall performance of the polymeric materials [26].

ZnO nanoparticles are non-toxic. They can be used to produce environmentally benign materials with excellent optical, chemical, thermal, mechanical and biological properties. They have versatile applications in different fields such as in transparent electronics, ultraviolet light emitters, photocatalysis, photo protecting devices, piezoelectric devices, chemical sensors, optoelectronic materials, spin electrics, UV-absorbing materials, cosmetics, along with antimicrobial and corrosion protective coating materials [13].

We selected virgin olive oil (VOO) for the synthesis of PUA and their ZnO nanocomposite. VOO is a non-drying oil (iodine value= 81, acid value=1.5 mg KOH/g, specific gravity at 27 °C=0.9133) obtained from olive seeds (olea europaea, family oleaceae), used in pharmaceuticals, cosmetics, and soaps. We developed polyetheramide from VOO for corrosion protective coatings [27]. In the present work we have synthesized VOO based polyurethanamide (OPUA) (curable at ambient temperature) and also polyurethane nanocomposite OPUA/ZnO coatings from VOO derived DFA (soft segment), TDI (hard segment) and different concentrations of ZnO nanoparticles (as filler) via microwave assisted method for their use as advanced coating material. The chemical structure, morphology, mechanical properties, thermal properties, and optical properties of OPUA/ZnO nanocomposites were investigated as a function of

†To whom correspondence should be addressed.
E-mail: malamiitd@gmail.com
Copyright by The Korean Institute of Chemical Engineers.

ZnO loading. A literature survey revealed that the modification of PUA derived from VO has been accomplished by inclusion of metal, metalloid, nanosilica, nanoclay; however, the modification of PUA with nano-ZnO has not been reported yet [9-12]. The present research work provides a synergistic approach towards the utilization of a renewable resource by an energy efficient pathway towards value addition; OPUA serves as the "greener" matrix while nano-ZnO as nanofiller provides reinforcement to the matrix, thus showing synergism.

EXPERIMENTAL

1. Materials

VOO (Turkey via Reef Corporation for Import and Export, Riyadh, KSA; fatty acid composition: oleic acid 80%, linoleic acid 5%, linolenic acid 1%, palmitic acid 10%) [27], diethanolamine (RiedeldeHaen, Germany), methanol, sodium metal, TDI (Acros Organics, USA) were used as received.

DFA of VOO, i.e., N-N′-bis(2-hydroxyl ethyl) olive oil fatty amide [HEOA] and ZnO nanoparticles used in the study were prepared by previously reported methods [27,28].

2. Synthesis of Olive Polyurethanamide (OPUA)

HEOA (0.10 mol) and TDI (1.0 mol) along with 8-10% xylene were taken in an Erlenmeyer flask. The reaction mixture was heated at 140±2 °C for 1 min under MW irradiations in a MW oven (MicroSYNTH PLUS, Milestone, Sorisole, BG, Italy). The completion of reaction was monitored by TLC and FTIR.

3. Synthesis of OPUA/ZnO Nanocomposite

10 gram of OPUA along with 20 ml xylene were placed in an Erlenmeyer flask and heated at 28±2 °C for 30 sec under MW irradiations and then ZnO (0.4 wt%, 0.6 wt% and 0.8 wt%) was added slowly. It was again heated at the same temperature for 2-3 min under MW irradiation. The synthesized systems are abbreviated as OPUA-0.4, OPUA-0.6 and OPUA-0.8. Last numeral indicates the wt% of ZnO w.r.t. OPUA.

TEST METHODS

FT-IR spectra of OPUA/ZnO nanocomposite were taken on an FT-IR spectrophotometer (Prestige-21, FTIR-8400S, Shimadzu Corporation, Kyoto, Japan) using NaCl cell. The thermal analysis was performed on TGA/DSC1 (Mettler Toledo AG, Analytical CH-8603 Schwerzenbach, Switzerland), at a heating rate of 10 °C/min in N_2 atmosphere. Molecular weight of OPUA resin was measured by GPC (HT-GPC Module 350A, Viscotek, Houston, TX, USA). Tetrahydrofuran was used as eluent at a flow rate 1.0 ml/min and calibrated with polystyrene standard. Refractive index was taken on Abbe Refractometer, Model R-4 Indian, Rajdhani Scientific Instrumets Co. India. Different compositions of OPUA/ZnO nanocomposite coatings were prepared using 40 wt% of OPUA/ZnO nanocomposite in solvent (xylene) by brush technique on commercially available mild steel (MS) strips of 30 mm×10 mm×1 mm for corrosion resistance and 70 mm×25 mm×1 mm for gloss test (ASTM D523-89) (Model RSPT20, Digital Instruments, Santa Barbara, California, USA) at 45°, scratch hardness (BS 3900), pencil hardness test (ASTM D3363) (Wolff-Wilborn tester, Sheen instruments, England), cross hatch adhesion test (ASTM D3359-02), impact resistance (IS; 101 part 5/sec-3, 1998), bend test (ASTM D 3281-84) and to measure the thickness of coatings by thickness gauge (Model 456, Elcometer Instrument, Manchester, UK). The nanocomposite was studied by Transmission Electron Microscope (JEM-2100F, Jeol, Japan). Scanning Electron micrographs (SEM) (JEOL, JSM 7600F, Japan) were taken for OPUA/ZnO coating and also OPUA/ZnO coating immersed in 5 wt% NaCl (240 hr), 3.5 wt% HCl (5 hr) and tap water (240 hr).

Potentiodynamic measurements were performed in three electrodes at room temperature, a platinum electrode as counter electrode, and saturated calomel electrode (SCE) as reference electrode. The specimen as working electrode was embedded by polytetera-fluroethylene (PTFE), exposed surface area of 1.0 cm^2 to different corrosive media 3.5 wt% HCl, 5 wt% NaCl and tap water (Cl^- ion 163.303 ppm, S^{2-} ion 139.375 ppm, Ca^{2+} ion 35.310 ppm measured by ICP Mass). Tafel curve were carried out using a computer-controlled Auto ACDSP (ACM Instruments) with Boukamp software. Potentiodynamic (Tafel) polarization curves were obtained using a sweep rate of 1 mV/s in the potential range of ±250 mV with respect to the initial open circuit potential. The linear Tafel segments of anodic and cathodic curve were extrapolated to corrosion potential to obtain the corrosion potential (E_{corr}), corrosion current density (I_{corr}), and inhibition efficiency (IE %). The IE of the coatings was calculated by the following equation [27].

$$\text{Inhibition Efficiency}\,(\%) = \frac{I_{0corr} - I_{corr}}{I_{0corr}} \times 100$$

where I_{0corr} and I_{corr} are corrosion current density of uncoated and coated MS.

RESULTS AND DISCUSSION

HEOA was prepared by amidation of Olive oil. The free hydroxyl groups of HEOA reacted with isocyanate groups of TDI by polyaddition reaction forming OPUA (Scheme 1) [6-12]. The polyurethane formation occurs in 1 minute by MW irradiation technique and in 2 hours by conventional heating [27]. The lowering of reaction time in former case is due to the interactions between materials and MW radiations. MW energy is directly delivered to the reaction mixture. Through molecular interactions with the electromagnetic field and heat generated by molecular collision and friction, the reaction is facilitated to occur at very low time period compared to conventional heating [29].

The strategy holds significance because of the following features: (i) using VO-a sustainable raw material, (ii) reaction occurring at lower temperature, (iii) obviating multi step reactions, and (iv) advocating value addition via "greener" route.

The molecular weight of OPUA was observed to be 5347 (Mw) and 3765 (Mn) with polydispersity Index as 1.420. Refractive index values were found to increase from HEOA (1.4903), OPUA-0.4 (1.5100), OPUA-0.6 (1.5108), to OPUA0.8 (1.5118) due to the presence of urethane linkages and metal oxide, respectively.

1. FTIR

Fig. 1 shows the FTIR spectrum of OPUA and OPUA-0.8. The OPUA spectrum shows characteristic peaks of polyurethane amide

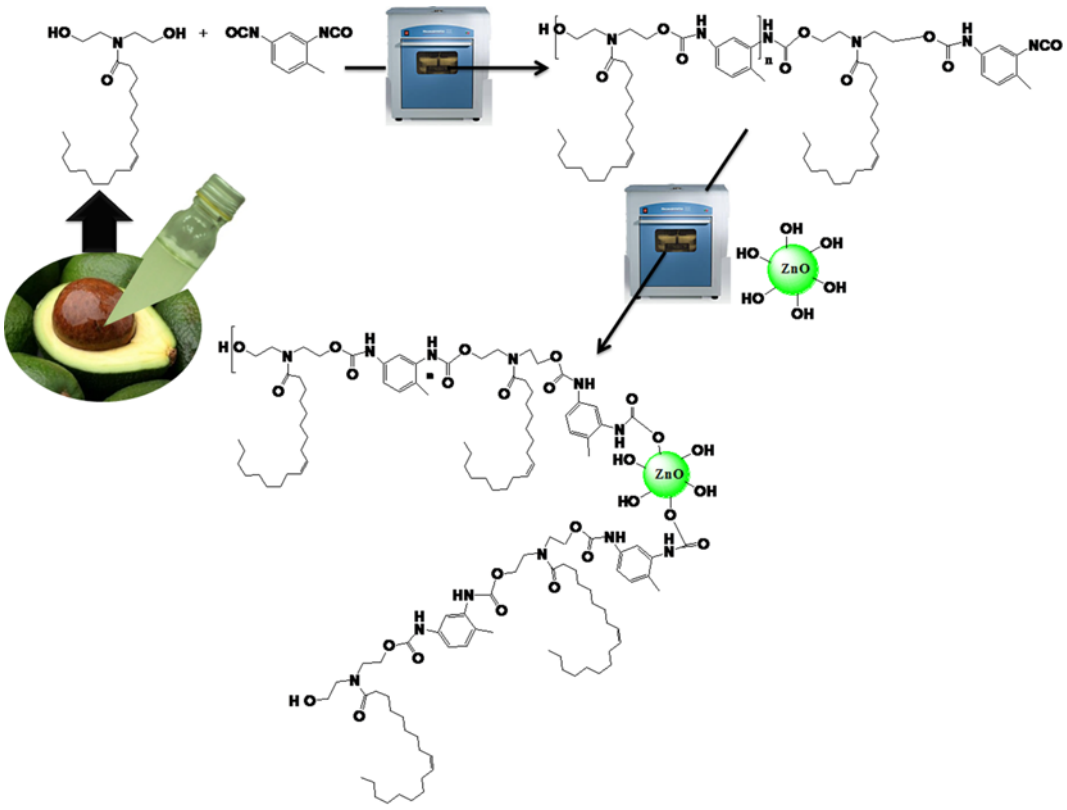

Scheme 1. Synthesis of OPUA/ZnO composite.

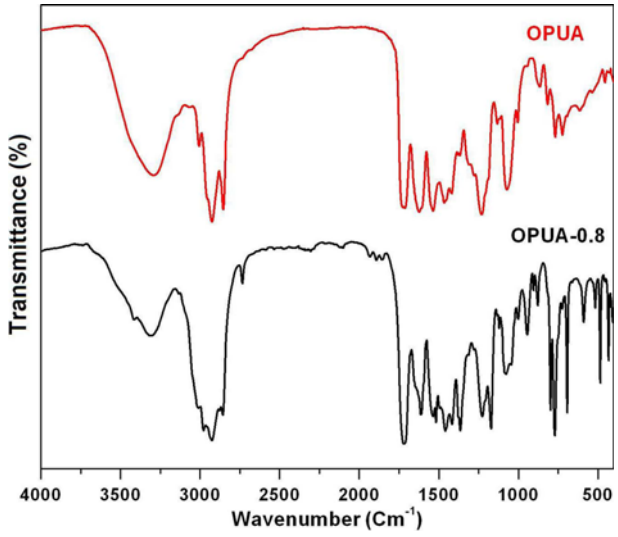

Fig. 1. FT IR spectra of OPUA and OPUA-0.8.

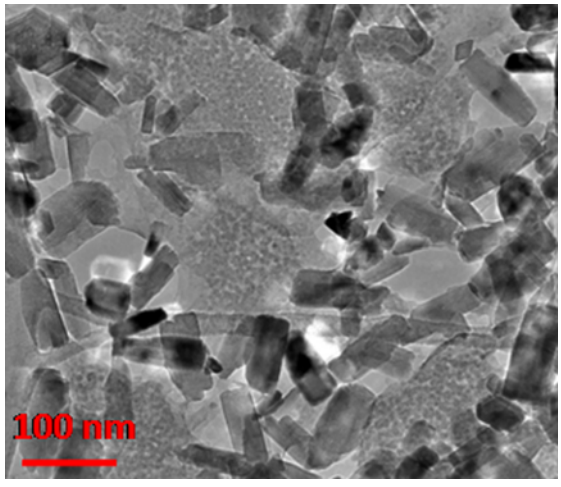

Fig. 2. TEM micrograph of ZnO nanoparticle in OPUA.

at 1,712 cm^{-1} (C=O urethane), 1,622 cm^{-1} (C=O amide), 2,273 cm^{-1} (t, free NCO), 1,230 cm^{-1} (NCOO-), 697 cm^{-1} (δ, very small peak N-H urethane). The spectrum of OPUA-0.8 also shows the other peaks characteristic of olive fatty amide chain in OPUA [6-12]. The spectrum of OPUA-0.8 shows some additional peaks, along with aforementioned peaks, at 3,422 cm^{-1} (OH of ZnO), and 589 cm^{-1}, 485 cm^{-1} (-O-Zn-O) [13]. Close examination of the spectrum of OPUA-0.8 reveals some shifting of peaks as in C=O urethane stretching peaks (+5 cm^{-1} shifting), C=O amide (–11 cm^{-1} shifting), and N-H urethane bending (–5 cm^{-1} shifting).

The presence of peaks at 3,422 cm^{-1} (OH of ZnO) and 589 cm^{-1}, 485 cm^{-1} (-O-Zn-O) can be correlated to the incorporation of nano-ZnO in OPUA, while the presence of sharp peaks at 692 cm^{-1} (δ, sharp N-H urethane) and disappearance of free NCO at 2,273 cm^{-1} can be correlated with the chemical reaction between surface -OH of nano-ZnO and free NCO groups of OPUA [6-13].

2. TEM Analysis

TEM micrograph (Fig. 2) clearly shows the presence of ZnO

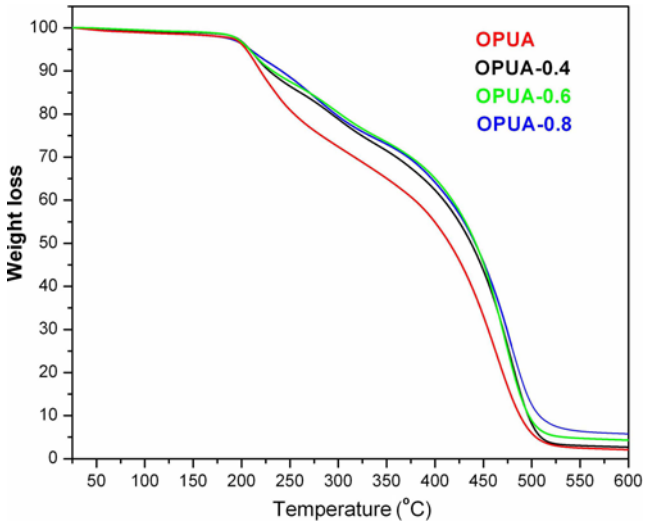

Fig. 3. TGA thermograms of OPUA, OPUA-04, OPUA-06, and OPUA-08.

nanoparticles in OPUA matrix. The particles are unagglomerated with distinct boundaries [28].

3. Thermal Analysis

Fig. 3 shows the TGA thermograms of OPUA, OPUA-0.4 OPUA-0.6 and OPUA-0.8. The thermal stability of nanocomposites increases with the incorporation of nano-ZnO. The initial weight loss (5% at loss) is observed at 200-210 °C in all systems. It can be correlated with evaporation of entrapped solvent. 10 to 20 wt% wt loss at 219-300 °C in virgin OPUA and nanocomposites is due to the degradation of urethane linkages [30,31]. 50 wt% loss at 436-440 °C in all compositions is attributed to the degradation of amide linkages. The amide linkages are more stable than urethane linkages. 80 wt% loss observed at 469-486 °C in all the compositions can be attributed to the degradation of hydrocarbons (aliphatic and aromatic). The increase of weight residue observed at 525 °C from OPUA to OPUA-0.8 can be related to the presence of ZnO nanoparticles.

DTA thermograms (Fig. 4) of OPUA, OPUA-0.4, OPUA-0.6, and OPUA-0.8 show three endotherms, while OPUA-0.8 shows two endotherms associated with good interactions between nanoparticles and the matrix in the latter. The endotherms at 313 °C, 342 °C, 341 °C and 340 °C can be attributed to the restructuring of segments or melting followed by degradation, the latter being evident in TGA thermogram within same temperature range. The nanocomposite coatings can be used safely up to 200-210 °C.

4. Physico-mechanical Performance

The coatings were cured at ambient temperature (30 °C). The cured specimens were subjected to physico-mechanical tests and corrosion studies after 30 days of their application over the substrate. The curing occurred by (i) solvent evaporation, (ii) reaction of free isocyanates with moisture as typical in polyurethane coatings, and (iii) auto-oxidation at unsaturation. The thickness of these coatings was found as 105±5 μm. The coatings showed good gloss (48), scratch hardness (2.0 kg), impact resistance (150 lb/inch), flexibility retention (1/8 inch conical mandrel) and pencil hardness values OPUA-0.4(3H), OPUA-0.6(5H), OPUA-0.8(5H). The coatings showed good cross hatch adhesion tape test, indicating good adhesion to the substrate contributed by polar hydroxyl, isocyanate, urethane, amide and ZnO nanoparticles.

5. Corrosion Studies

Fig. 5 shows the potentiodynamic polarization curve of bare MS, OPUA-0.4, OPUA-0.6 and OPUA-0.8 after 240 h immersion in 3.5% HCl solution. The corrosion potential (E_{corr}) of bare MS moves to more noble values from −539.59 to −512.15, −447.25 and −384.80 mV vs. calomel reference electrode. The presence of ZnO nanoparticles polarizes the E_{corr} in the same direction. As can be seen in Table 1, the inhibition efficiency of composite coatings is greater than bare MS in acidic medium. Fig. 6 shows the polarization curve in 5% NaCl after 240 h immersion; the corrosion potential as well as corrosion current density decrease from bare MS to OPUA-0.8 (Table 1). Fig. 7 represents the polarization curve in tap water after 252 h immersion. I_{corr} of bare MS was 4.211×10^{-2} mA/cm^3 and E_{corr} −679.87 mV. As compared to OPUA-0.4 and OPUA-0.6, OPUA-

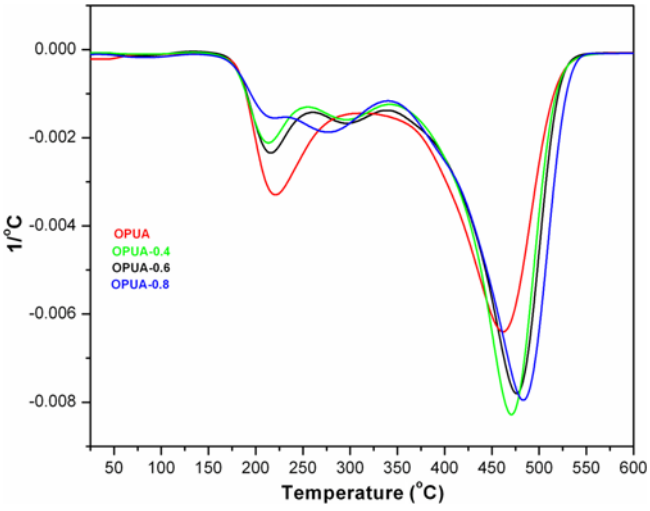

Fig. 4. DTA thermogram of OPUA, OPUA-04, OPUA-06, and OPUA-08.

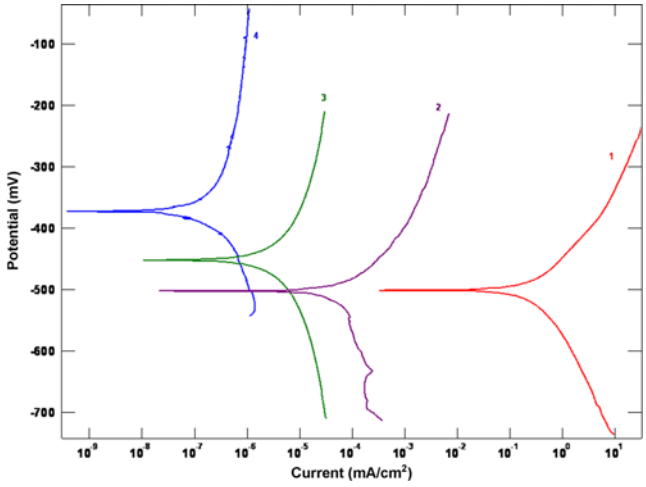

Fig. 5. Tafel plots of (1) MS, (2) OPUA-04, (3) OPUA-06, and (4) OPUA-08 coated in HCl solution.

Table 1. Corrosion parameters for coated and bare mild steel in different corrosive environment

*Code	Medium	βa	βc	E_{corr} (mV)	I_{corr} (mA/cm^3)	Corrosion rate (mm/yr)	Inhibition efficiency (%)
MS	3.5%HCl	171.72	163.18	−539.59	1.8487	21.426	-
OPUA-0.4	3.5%HCl	230.04	257.02	−512.15	6.63×10^{-4}	7.693×10^{-3}	99.96
OPUA-0.6	3.5%HCl	413.50	433.20	−447.25	1.18×10^{-5}	1.296×10^{-4}	99.99
OPUA-0.8	3.5%HCl	675.17	231.57	−384.80	3.79×10^{-7}	4.403×10^{-6}	99.99
MS	5%NaCl	55.84	596.00	−550.83	1.3485	15.629	-
OPUA-0.4	5%NaCl	528.70	402.48	−606.37	5.777×10^{-3}	6.695×10^{-2}	99.57
OPUA-0.6	5%NaCl	308.53	324.92	−596.73	1.043×10^{-3}	1.209×10^{-2}	99.99
OPUA-0.8	5%NaCl	488.69	347.92	−110.54	1.852×10^{-6}	2.147×10^{-5}	99.99
MS	Tap water	200.99	1112.3	−679.87	4.211×10^{-2}	0.488	-
OPUA-0.4	Tap water	278.91	534.43	−706.96	5.353×10^{-4}	6.204×10^{-3}	98.72
OPUA-0.6	Tap water	368.09	283.48	−625.93	2.300×10^{-6}	1.507×10^{-5}	99.94
OPUA-0.8	Tap water	382.15	396.00	158.28	1.393×10^{-6}	2.393×10^{-5}	99.94

*Sample code: MS>Bare Mild Steel

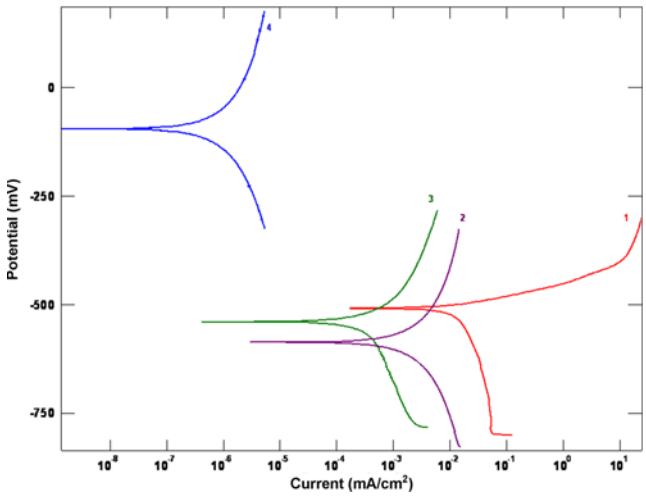

Fig. 6. Tafel plots of (1) MS, (2) OPUA-04, (3) OPUA-06, and (4) OPUA-08 coated in NaCl solution.

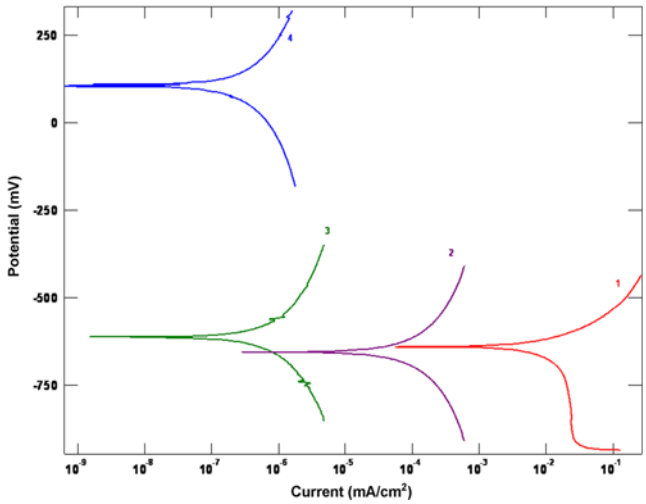

Fig. 7. Tafel plots of (1) MS, (2) OPUA-04, (3) OPUA-06, and (4) OPUA-08 coated in Tap water.

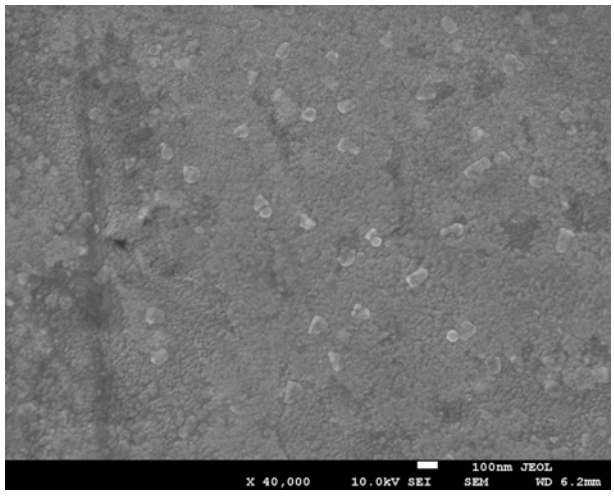

Fig. 8. SEM micrograph of OPUA-0.8.

0.8 has smaller I_{corr} value, 1.393×10^{-6}, which shows that 0.8% ZnO nanoparticle containing OPUA has better protection than others. OPUA-0.8 shows higher inhibition efficiency against the attack of corrosive media. These results demonstrate that ZnO nanoparticle containing OPUA coating acts as a protective layer on mild steel to improve the corrosion protection performance. The biocomposites produced compact and uniform, hydrophobic and impermeable covering (barrier) at the interface of the substrate and corrosive media, hindering the permeation of corrosive ions.

6. SEM Analysis

SEM micrographs (Fig. 8) of composite coatings show the presence of ZnO in OPUA matrix. The micrograph (Fig. 9) of NaCl tested coating shows that the coating is unaffected in saline environment; slight deposition of salt is evident on the surface. After being subjected to acidic environment, the micrograph (Fig. 10) shows the presence of cracks on the coating surface. However, the said medium is unable to penetrate the coating and reach the substrate, i.e., the coating does not lose adhesion with the substrate and shows no dissolution or further deterioration. The micrograph

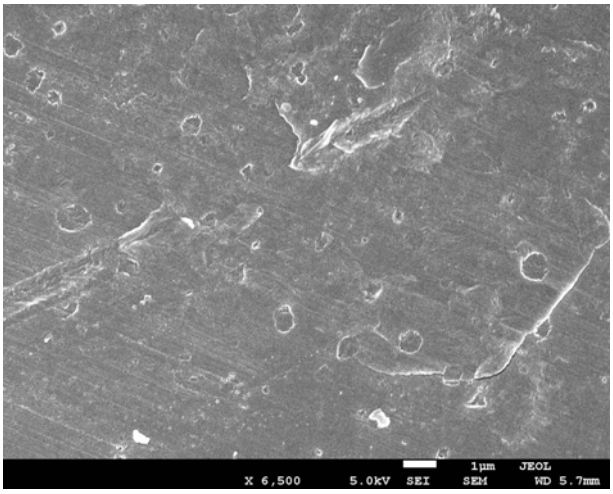

Fig. 9. SEM micrograph of OPUA-0.8 after immersion in NaCl solution.

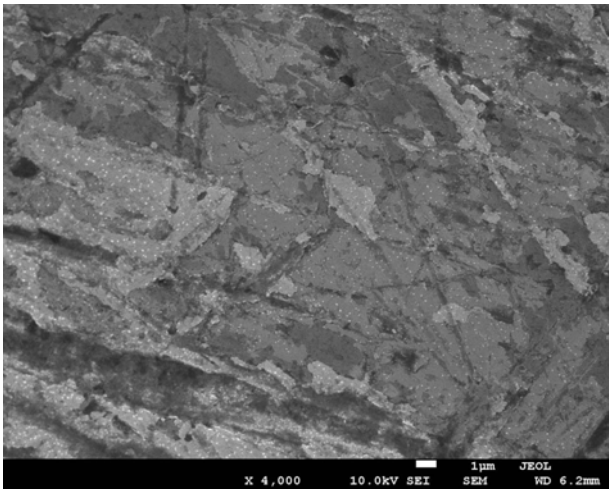

Fig. 10. SEM micrograph of OPUA-0.8 after immersion in HCl solution.

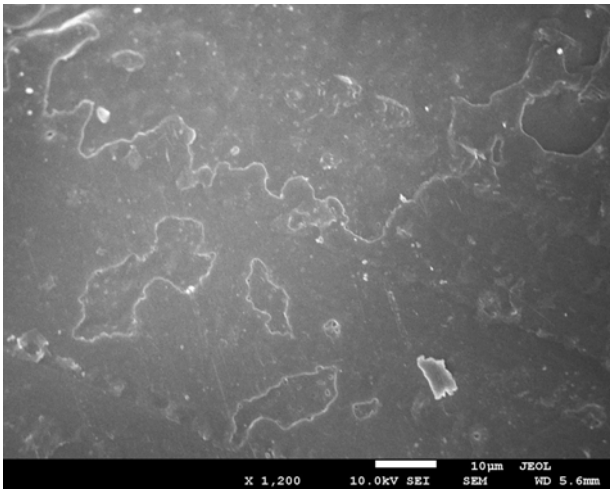

Fig. 11. SEM micrograph of OPUA-0.8 after immersion in Tap water.

(Fig. 11) of the sample dipped in tap water shows that the coating is unaffected, however accompanied by slight loss in gloss.

CONCLUSION

Olive oil polyurethanamide/ZnO coatings were prepared by simple chemical approach at lower reaction temperature, within lower reaction time, via simple curing strategy. The corrosion protection mechanism is based upon the barrier action of coatings upon the substrate, due to good adhesion conferred by polar hydroxyl, urethane, amide groups as well as hydroxyls present on ZnO surface. The coatings showed good physico-mechanical performance and corrosion protection in various corrosive media (5 wt% NaCl, 3.5 wt% HCl, and tap water). The approach may be well employed on those oils that are not utilized or find limited utilization till date.

ACKNOWLEDGEMENTS

The Project was supported by King Saud University, Deanship of Scientific Research, College of Science - Research Centre.

REFERENCES

1. V. Sharma and P. P. Kundu, *Prog. Polym. Sci.*, **33**, 1199 (2008).
2. F. S. Guner, Y. Yagci and A. T. Erciyes, *Prog. Polym. Sci.*, **31**, 633 (2006).
3. M. Alam, D. Akram, E. Sharmin, F. Zafar and S. Ahmad, *Arab. J. Chem.*, **7**, 469 (2014).
4. E. Sharmin, F. Zafar, D. Akram, M. Alam and S. Ahmad, *Ind. Crops Prod.*, **76**, 215 (2015).
5. S. Dutta and N. Karak, *Prog. Org. Coat.*, **53**, 147 (2005).
6. S Yadav, F. Zafar, A. Hasnat and S. Ahmad, *Prog. Org. Coat.*, **64**, 27 (2009).
7. M. Kashif, F. Zafar and S. Ahmad, *J. Appl. Polym. Sci.*, **117**, 1245 (2010).
8. M. Kashif, E. Shamin, F. Zafar and S. Ahmad, *J. Am Oil Chem. Soc.*, **88**, 1989 (2011).
9. F. Zafar, M. Kashif, E. Sharmin and S. Ahmad, *Macrol. Symp.*, **290**, 79 (2010).
10. S. Ahmad, F. Zafar, E. Sharmin, N. Garg and M. Kashif, *Prog. Org. Coat.*, **73**, 112 (2012).
11. F. Zafar, M. H. Mir, M. Kashif, E. Sharmin and S. Ahmad, *J. Inorganic Organometallic Polym. Mater.*, **21**, 61 (2011).
12. F. Zafar, H. Zafar and E. Sharmin, *J. Appl. Polym. Sci.*, **131**, 40278 (2014).
13. E. Sharmin, O. Rehman, F. Zafar, D. Akram, M. Alam and S. Ahmad, *RSC Adv.*, **5**, 47928 (2015).
14. S. K. Dhoke and A. S. Khanna, *Corros. Sci.*, **51**, 6 (2009).
15. M. G. Sari, B. Ramezanzadeh, M. Shahbazi and A. S. Pakdel, *Corros. Sci.*, **92**, 162 (2015).
16. X. Komman, L. A. Berglund, J. Sterte and E. P. Giannelis, *Polym. Eng. Sci.*, **38**, 1351 (1998).
17. A. Farbod, G. M. Parvinzadeh, S. Ali and K. Amir, *Superlattices Microstruct.*, **52**, 50 (2012).
18. S. S. Golru, M. M. Attar and B. Ramezanzadeh, *Prog. Org. Coat.*, **77**, 1391 (2014).

19. S. Mallakpour and M. Dinari, *Prog. Org. Coat.*, **75**, 173 (2012).
20. M. R. Shaik, M. Alam and N. M. Alandis, *J. Nanomater*, **2015**, Article ID 745217 (2015).
21. M. P. Gashti, A. Almasian and M. P. Gashti, *Sensor Actuat-A Phys*, **187**, 1 (2012).
22. M. Parvinzadeh and S. Eslami, *Res. Chem. Intermed.*, **37**, 771 (2011).
23. L. K. Joy, V. Sooraj, U. S. Sajeev, S. S. Nair, T. N. Narayanan, N. Sethulakshmi, P. M. Ajayan and M. R. Anantharaman, *Appl. Phys. Lett.*, **104**, 121603 (2014).
24. A. Dey, S. Panja, A. K. Sikder and S. Chattopadhyay, *RSC Adv.*, **5**, 10358 (2015).
25. M. P. Gashti and A. Almasian, *Composites Part B*, **45**, 282 (2013).
26. T. O. Siyanbola, K. Sasidhar, B. Anjaneyulu, K. P. Kumar, B. V. S. K. Rao, R. Narayan, O. Olaofe, E. T. Akintayo and K. V. S. N. Raju, *J. Mater. Sci.*, **48**, 8215 (2013).
27. M. Alam and N. M. Alandis, *Prog. Org. Coat.*, **75**, 527 (2012).
28. M. Alam, N. M. Alandis, A. A. Ansari and M. R. Shaik, *J. Nanomater*, **2013**, Article ID 157810 (2013).
29. R. Hoogenboon and U. S. Schubert, *Macromol. Rapid Commun.*, **28**, 368 (2007).
30. M. Alam, E. Sharmin, S. M. Ashraf and S. Ahmad, *Prog. Org. Coat.*, **50**, 224 (2004).
31. P. D. Meshram, R. G. Puri, A. L. Patil and V. V. Gite, *J. Coat. Technol. Res.*, **10**, 331 (2013).